
QLENS: Towards A Quantum Perspective of Language Transformers

Aditya Gupta
Issaquah High School
Washington, USA
aditya441g@gmail.com

Kirandeep Kaur, Vinayak Gupta
University of Washington
Washington, USA
kaur13@uw.edu, guptavinayak51@gmail.com

Abstract

In natural language processing, current methods for understanding Transformers are successful at identifying intermediate predictions during a model’s inference. However, these approaches function as limited diagnostic checkpoints, lacking a mathematical framework for mechanistically modeling how each layer facilitates transitions between these evolving states. This interpretability gap and past successes of interdisciplinary outlooks inspire us to turn to physics in search of a descriptive mathematical framework for Transformers. We observe that language models are intrinsically probabilistic, an attribute that is echoed in the core postulates of quantum mechanics. This parallel inspires us to translate insights from this discipline to that of natural language processing. Towards this objective, we propose QLENS a novel attempt to develop a physics-based perspective on the Transformer generation process. Under QLENS, a Transformer is studied by converting its latent activations into a state vector in a Hilbert space derived from the model’s output units. This state subsequently evolves through hidden layers—reformulated as unitary operators and analogously defined Hamiltonians—during inference. The model’s final probability distribution is obtained by applying the Born rule to the end state using a specific measurement operator. To demonstrate QLENS’s potential, we conduct a proof-of-concept by probing a toy Transformer to investigate the influence of individual layers in a model’s prediction trajectory. We present our work as a foundation for cross-domain insights to be leveraged towards a broader understanding of Transformers.

Our paper presents a preliminary framework to model probability flow and interactions within a Transformer. While it offers an initial perspective on the interpretability problem, we are willing to update our claims if significant issues are discovered.

1 Introduction

Probabilistic distributions lie at the heart of Transformers [50]. These neural networks iteratively transform their residual stream, gradually converging on a hidden state which can be mapped to prediction probabilities. This architecture has proven to be remarkably effective at generalizing across statistical variations in real-world data [9], accommodating them by learning distinct prediction trajectories. Yet this intrinsic integration of probability is not restricted to these SOTA models; it also plays a central role in the universe, notably through its incorporation into quantum mechanics (QM). This branch of physics reveals that particle measurements follow a distribution derived from a temporarily evolving wavefunction, where each observation’s result is obtained at random, consistent with the final distribution. These parallels suggest that cross-domain insights from QM could be

leveraged to provide a novel perspective of Transformers by formalizing their layer-by-layer refinement trajectories.

Current approaches to interpretability have provided established tools for iterative inference [24] in natural language processing (NLP) Transformers, which are the focus of this work. Prominently, the Logit Lens [36] has emerged as a prominent model that uses the final layer of a Transformer to extract its intermediate predictions during inference. Although the original lens was found to be a biased estimator of final outputs, Belrose et al. improved its design by incorporating a tunable constant term to account for the average residual update learned by the model [4]. Their Tuned Lens method has facilitated the analysis of example difficulty [4], epistemic uncertainty in prediction trajectories [28], and stages of inference [30] in attention-based Transformers. However, while the Tuned Lens is a functional diagnostic tool for identifying various points that comprise a model’s prediction trajectory, it lacks a mathematical model for studying how individual layers facilitate transitions along this path.

To make inroads towards overcoming this difficulty, we turn to physics for inspiration, a subject that has repeatedly proven suitable for providing cohesive theoretical backbones for observable phenomena. Whereas previous efforts to unite physics with interpretability studies have been largely reserved to its classical branches [33, 5], we propose a novel QM-inspired perspective. Our Quantum Lens (QLENS) establishes a quantum-mechanical analogy for Transformers, providing a mathematical framework to model layer transitions. By formalizing the prediction path as a sequence of unitary state evolutions, QLENS moves beyond the capabilities of the Tuned Lens to mechanistically characterize how each layer contributes to the final output probability distribution. We then apply this analogy to a toy classification Transformer, illustrating that QLENS can mathematically describe the effect of each layer in the output space and derive insights from the resulting data.

To ground the methodology of QLENS, we begin by deriving the closest equivalents of quantum mechanical postulates in the context of Transformers. We illustrate that the output space of a Transformer can be converted to an analogous orthonormal Hilbert basis for the model, with each output unit corresponding to a distinct state that a Transformer can produce. Exercising this framing, QLENS views a Transformer’s latent representation as specifying a *state vector*, using which the probability distribution for subsequent tokens can be tracked during inference. Transformer layers then are formulated as *unitary operators* evolving their input state vectors according to the Schrödinger equation. This framework enables the definition of a corresponding *Hamiltonian* for each layer, which provides a dual perspective of layers that aligns with residual addition. The final output distribution is extracted from the last state vector through a dedicated *measurement operator* via the Born rule, formalizing the probabilistic foundations of Transformers.

With these analogies, QLENS institutes a theoretical basis to translate the QM formulations to NLP Transformers. Our work both elicits conceptual parallels between these two disciplines and identifies the open areas in which the ties between the two fields may be strengthened. Through this fresh approach, we hope to open a promising pathway towards a more profound understanding of Transformers. Our key contributions are summarized below:

1. We demonstrate the thematic resemblance between QM and Transformers, uncovering the nearest equivalents of the postulates of QM in this domain.
2. Through these definitions, we propose QLENS, an end-to-end quantum mechanical analogy of the Transformer inference process.
3. We demonstrate proof of concept by applying QLENS to interpret the layers of a simple sentiment classification Transformer.
4. We critically analyze the current strengths and limitations of QLENS to promote further exploration of this novel perspective of Transformer.

2 Related Work

Interpretability is the procedure of converting one explanation of a concept into another, more human-understandable form [54, 18]. As neural network architectures increasingly scale [38, 9, 17], it has become necessary to establish a conceptual grasp of these models to ensure model faithfulness beyond performance metrics [10]. Present approaches to interpretability include classifier-based probes [25], activation explanation [14, 39], and mechanistic interpretability with circuits [7, 13].

Jawahar et al. (2019) [25] train a linear probe to categorize BERT [16] outputs by linguistic features of interest. Their findings reveal that layers at different positions in BERT’s Transformer architecture specialize to various levels of linguistic characteristics: earlier layers identify surface-level syntactic patterns while later ones surface semantic concepts. Dalvi et al. (2018) [14] adopt a more fine-grained methodology, where classifiers are trained to determine correlations between neuron activations and the presence of lexical structures, illustrating that individual directions in the model’s latent space can represent specific properties. Bricken et al. (2023) [7] observe the challenge of polysemanticity—where individual neurons respond to multiple distinct combinations of inputs—and instead use sparse autoencoders to display that groups of neurons and their connections across various layers form circuits to capture semantic features. However, these low-level methods localize to a limited range of behaviors and do not explain information flow through the model as a whole. In contrast, we argue that procedures based on physical analogies can more holistically achieve the goal of interpretability by adopting an overarching theoretical viewpoint to reframe the complex workings of Transformers in the context of well-studied natural phenomena.

Integrating physics into machine learning is an idea that returns to the roots of the latter field. Prominently, Hopfield networks [22] use a Hebbian learning algorithm to train a collection of neurons to store a desired memory in the form of bits. The state of the network at any time is associated with a particular energy function that derives from the Ising models of statistical mechanics. These networks themselves are only a subset of the generalized group of Boltzmann machines [1]. Although such physics-inspired model frameworks are valuable for their inherently interpretable design, their specific architecture requirements and symmetric weight matrices limit the applicability of their insights to the current state-of-the-art Transformers despite contemporary breakthroughs [41].

Recently, physics has been translated to probe the depths of more modern models and garner insights regarding their internal processes. Large language model (LLM) training dynamics have been explored from the perspectives of both thermodynamics [33] and classical mechanics [5], demonstrating that laws paralleling those that govern the universe may be fundamental to the learning process. In comparison to classical physics, however, the applications of quantum mechanics towards developing a comprehensive understanding of Transformer functions have been sparsely explored. Current interdisciplinary works between these two domains have primarily fallen under the quantum machine learning (QML) [27] or machine learning for quantum mechanics (ML4QM) [15] paradigm. QML aims to harness potential computational advantages wrought by quantum computers for training [29] and implementing [12, 11, 32] Transformers efficiently. Conversely, ML4QM uses Transformers as a problem-solving tool in QM, applying it to simulate the complex dynamics of multi-particle systems [53, 31]. Contrary to these approaches, we propose using QM as a mathematical framework to sequentially examine Transformer layers and explain the process towards Transformers converge on their outputs. In doing so, we uncover novel analogies for the forward pass of the generation process and ground future work in this nascent area of quantum-inspired interpretability.

3 Background

QLENS lies at an intersection of QM, NLP Transformers, and the Tuned Lens. To lay the groundwork for it, we outline the central tenets of each of these domains in this section. The founding postulates of quantum mechanics provide the language through which QLENS is developed, while the structure of the Transformer paradigm establishes the mold into which it integrates. By using the Tuned Lens as a bridge between the two, QLENS synthesizes a novel mathematical perspective towards conceptualizing Transformers.

3.1 Quantum Mechanics

Emerging at the start of the twentieth century [6, 26] and rapidly progressing in the 1920s and 1930s, QM reshaped the deterministic view held by most prominent physicists of the time. Led by figures such as Max Planck, Niels Bohr, Erwin Schrödinger, and Werner Heisenberg, the quantum revolution established a new probabilistic formulation of physics. We review the basics of this theory to prepare for its implementation in QLENS.

Rather than possessing a definite state, quantum particles exist in a *superposition* of multiple states until a measurement takes place. The space of possible states is described by a complex Hilbert

space $\mathcal{H} = \mathbb{C}^n$, with each of the n mutually orthonormal basis vectors $|a, b, c, \dots\rangle$ specifying it representing a distinct state. The information of a quantum system is captured in its *state vector* $|\Psi\rangle \in \mathbb{C}^n$. The state vector can be expanded in terms of the basis vectors,

$$|\Psi\rangle = \sum_{a,b,c,\dots} \psi(a, b, c, \dots) |a, b, c, \dots\rangle,$$

with the coefficients $\psi(a, b, c, \dots)$ designate the *wavefunction* of the system. The state vector is normalized, which places the restriction

$$\sum_{a,b,c,\dots} \psi^*(a, b, c, \dots) \psi(a, b, c, \dots) = 1$$

on the wavefunction.

When a particle is in a known state $|\Psi\rangle$, quantum mechanics accurately predicts the outcomes of possible experimental measurements that can be performed on it. These measured quantities, or *observables*, are represented by linear Hermitian operators \mathbf{L} . When expressed in a particular basis, these operators take the form of matrices with elements given by:

$$m_{kj} = \langle k | \mathbf{L} | j \rangle,$$

where $|k\rangle$ and $|j\rangle$ are basis vectors. The complete expansion of \mathbf{L} is given by computing m_{kj} over all possible pairs of basis vectors.

The possible results of a measurement are the eigenvalues λ_i of its corresponding operator \mathbf{L} . The state vector for which the result of the measurement to be *guaranteed* to be λ_i is the related unit eigenvector $|\lambda_i\rangle$. However, in general, the outcome of each measurement of $|\Psi\rangle$ is probabilistic, with the likelihood P to observe λ_i given by the Born rule:

$$P(\lambda_i) = \langle \lambda_i | \Psi \rangle \langle \Psi | \lambda_i \rangle = |\langle \lambda_i | \Psi \rangle|^2.$$

It follows that the state vector represents the probability distribution of a particle’s measurement outcomes. In between measurements, the state vector, and likewise this distribution, evolves over time as described by the time-dependent Schrödinger equation:

$$\hbar \frac{\partial |\Psi\rangle}{\partial t} = -i\mathbf{H} |\Psi\rangle.$$

Here, \mathbf{H} is a Hermitian operator known as the *Hamiltonian*, which represents the energy of the system; its eigenvalues are the allowed energy levels of the system. The physical constant \hbar is the *reduced Planck’s constant*, with value $\hbar \approx 1.055 \times 10^{-34} \text{ J} \cdot \text{s}$. Importantly, the state at any time t can be written as

$$|\Psi(t)\rangle = \mathbf{U}(t) |\Psi(0)\rangle,$$

with $|\Psi(0)\rangle$ being the initial state of the system and $\mathbf{U}(t)$ being a particular time-dependent unitary linear operator (satisfying $U^\dagger(t)U(t) = I$) known as the *time-development operator*, which is found by solving the Schrödinger equation [49, 51].

Notably, both Hamiltonians and unitary operators express the process of temporal evolution in QM. In QLENS, we maintain the quantum relationships between Transformer analogs of these quantities to leverage the preexisting mathematical structure of QM in our exploration. This permits QLENS to fluidly transition between synonymous quantum descriptions of an underlying physical behavior, unearthing twin quantum mechanical viewpoints of Transformers, each with their own distinct advantages. We examine this dualism in detail in sections 4 and 5, tracing it from its theoretical roots to its practical application.

3.2 Attention-Based NLP Transformers

SOTA NLP models are predominately initialized with a Transformer-based architecture. In this paper, we focus on attention-based Transformers to extend the Tuned Lens [4] formulation with a quantum-inspired approach to interpretability. These deep neural networks learn a set of weights through gradient descent during training [43] that allows them to carry out tasks such as text generation and sentiment classification. To prepare for investigating the dynamics of the layers of this design in QLENS, we present an overview of this structure in this subsection.

At a high level, inference from an attention-based Transformer [50] can be broken into 3 general phases: tokenization and embedding, hidden layers, followed by unembedding and sampling. We revisit each in order of their execution to familiarize ourselves with their standard implementation.

3.2.1 Step 1: Tokenization and Embedding

When supplied a text sequence, a Transformer begins by splitting its contents into discrete character combinations, called tokens. The set of all possible tokens $T = \{t_1, t_2, t_3, \dots, t_V\}$ is known as the model’s vocabulary, with V being its cardinality. This set can contain words, subwords, and even special start and end tokens (among others) to guide the model’s response. Tokenization produces an effective input token sequence $I_n = \{i_1, i_2, i_3, \dots, i_n\}$, where n is the length of the tokenized input. Each of these input tokens is then assigned to a D -dimensional embedding vector $x_i \in \mathbb{R}^D$ via two matrices: an embedding matrix $W_E \in \mathbb{R}^{V \times D}$ and a positional embedding matrix $W_{PE} \in \mathbb{R}^{n \times D}$. These embedding vectors are designed to capture semantic information [34] in the model’s latent space and are gradually refined in the next stage of this procedure.

3.2.2 Step 2: Hidden layers

These layers, comprising the bulk of a model’s parameters, are classified into two types of alternating operations which are repeatedly performed: *multi-layer perceptrons* and *multi-headed attention*. We begin by defining notation to assist in our exploration. Let x_i^ℓ denote the hidden state of the i -th token’s embedding vector after processing by ℓ Transformer layers. To represent these i vectors in a more compact form, they are bundled into a single residual stream matrix $X^\ell \in \mathbb{R}^{n \times D}$, where the i -th row of this matrix contains x_i^ℓ . The ℓ -th layer is then a function $f^\ell : \mathbb{R}^{n \times D} \rightarrow \mathbb{R}^{n \times D}$ that acts on X^ℓ . The nuances of these layers are described below.

Multi-Layer Perceptron (MLP): An MLP layer is a feedforward neural network consisting of two groups of fully connected perceptrons [42] with a nonlinear activation function in between. Mathematically, these layers can be characterized by the equation

$$X^{\ell+1} = X^\ell + [g(X^\ell W_\uparrow^\ell + b_\uparrow^\ell)] W_\downarrow^\ell + b_\downarrow^\ell,$$

which illustrates the conjunction of three successive transformations whose output is added to the residual stream at the layer’s conclusion. First, an affine transformation designated by the weight matrix $W_\uparrow^\ell \in \mathbb{R}^{D \times P}$ and bias $b_\uparrow^\ell \in \mathbb{R}^P$ projects X^ℓ into a P -dimensional feature space, with $P > D$. The output matrix is subsequently passed through a non-linear activation function $g(\cdot)$. Finally, a down-projection back to the embedding space is performed, denoted by the matrix $W_\downarrow^\ell \in \mathbb{R}^{P \times D}$ and the bias $b_\downarrow^\ell \in \mathbb{R}^D$. The result is then summed with the input X^ℓ to prepare the residual stream state $X^{\ell+1}$ for the next layer of the model [47].

Multi-headed Attention: While the principles behind MLPs emerged in the late 1950s, attention is a comparatively recent discovery that has helped drive the current rapid pace of model development. In their seminal work, Vaswani et al. introduced multi-headed attention [50], which unlike MLPs allow hidden state vectors to *attend* or pass information between one another. As implied by the name, multi-headed attention layer consists of multiple *heads* or modules within which a scaled dot-product attention operation is carried out. Concretely, if a layer has h heads and receives the input matrix X^ℓ as above, then the output of the j -th head is given by

$$\text{Attention}(Q_j, K_j, V_j) = \sigma \left(M + \frac{Q_j K_j^\top}{\sqrt{d_k}} \right) V_j,$$

where $Q_j = X^\ell W_j^Q$, $K_j = X^\ell W_j^K$, and $V_j = X^\ell W_j^V$ are known as the *queries*, *keys*, and *values* respectively. The weight matrices W_j^Q , W_j^K , $W_j^V \in \mathbb{R}^{D \times d_k}$ derive Q_j , K_j , and V_j from X^ℓ by down-projecting it into a smaller *key-query-value space* with dimensionality $d_k < D$. As $Q_j, K_j, V_j \in \mathbb{R}^{n \times d_k}$, the i -th row of each matrix is the query q_i , key k_i , or value v_i that is obtained from the input vector x_i^ℓ . The term $Q_j K_j^\top$ is a matrix of *attention weights* between the queries and keys of the input vectors, where each entry w_{ab} is calculated by taking the dot product between the query q_a of x_a^ℓ and the key k_b of x_b^ℓ for $a, b \in \mathbb{Z}, 1 \leq a, b \leq n$. Higher-valued entries indicate that the vector x_a^ℓ attends more to x_b^ℓ , which can be interpreted as demonstrating that x_a^ℓ is particularly relevant to updating the semantic content of x_b^ℓ . For numerical stability, the scaling factor $\sqrt{d_k}$ is incorporated. In certain NLP tasks, the attention weight matrix is then added to a masking matrix M , which prevents later tokens from attending to those earlier in the sequence, to improve the effectiveness of training. These attention weights are normalized via the softmax function $\sigma(\cdot)$ and are used to rescale the components of V_j . The i -th row of this modified value matrix describes how

the head should revise each vector x_i^ℓ . However, the dimensionality of these row vectors is d_k and thus cannot be directly added to x_i^ℓ . As a result, once each attention head’s result is procured, multi-head attention up-projects each V_j back to the embedding space. For computational efficiency, this is accomplished by concatenating the results of each head and then multiplying them by an output matrix $W^O \in \mathbb{R}^{hd_k \times D}$, culminating in the formulation:

$$\text{MultiHead}(Q, K, V) = \text{Concat}(\text{head}_1, \text{head}_2, \dots, \text{head}_h)W^O.$$

Likewise to the MLP layers, the output of multi-headed attention is added to X^ℓ to form the input to the next layer [46].

$$X^{\ell+1} = X^\ell + \text{MultiHead}^\ell(Q, K, V).$$

Note: While MLP’s and multi-headed attention form the core of a Transformer’s layers, between these main constituents the residual stream is additionally transformed by residual connections [20] and layer normalization [3]. While these components are useful in training to avoid vanishing gradients, these technical points are omitted here for the purpose of conceptual clarity.

3.2.3 Step 3: Unembedding and Sampling

After the final hidden layer L has been incorporated into the residual stream to produce X^{L+1} , the model converts its hidden state into a prediction for the next token o_{n+1} . This hidden state can be decomposed row-wise into the set of token states $H^{L+1} = \{x_i^{L+1} | i \in \mathbb{Z}, 1 \leq i \leq n\}$. A task-specific selection function $S(\cdot)$ then chooses one of these states h_{out} to be used by the prediction head:

$$h_{\text{out}} = S(H^{L+1}) \quad \text{where } h_{\text{out}} \in \mathbb{R}^D.$$

For instance, LLMs commonly select the last token x_n^L for next-token prediction, while text classification tasks use the hidden state of the special classification token. Once, h_{out} is extracted, it is mapped to a *logit vector* $v \in \mathbb{R}^N$ through an unembedding matrix $W_U \in \mathbb{R}^{D \times N}$ and bias $b_U \in \mathbb{R}^N$, where N is the number of output units of the Transformer (e.g. individual tokens for LLMs, text classes such as positive and negative for NLP classification tasks). The entries of this vector are unnormalized scores for each of the possible outputs in the set of output units $C = \{c_1, c_2, c_3, \dots, c_N\}$. The logit vector is then recast into a probability distribution θ for these tokens through softmax. The output c_{out} can then be derived from this distribution:

$$\theta = \sigma(v) = \sigma(x_n^L W_U + b_U),$$

$$c_{\text{out}} \sim \theta.$$

While models often have task-specific alterations, the procedure outlined in eqs. 3.2.1 to 3.2.3 is at the heart of all NLP Transformers. In QLENS, this process is reconstructed with insights from QM, where these three stages of Transformer are viewed as establishing a basis for the analogous state vector of the model, evolving the wave function of this vector, and finally observing it to probabilistically collapse it to a distinct state. This foundation allows QLENS to supply QM-based insights for components of the Transformer paradigm, applicable across the diversity of its deployment tasks.

3.3 The Tuned Lens

While the evolution of quantum states can be viewed as the updating of a probability distribution, this concept does not translate directly to Transformers. This is because Transformer layers refine abstract hidden states, with a distribution typically only extracted in the last layer. To resolve this distinction, QLENS employs the Tuned Lens [4], a probe designed to translate intermediate hidden states into prediction logits. Normalizing these logits produces an output distribution, allowing the trajectory of a Transformer’s output probabilities to be tracked. We review this tool in this section, beginning from its roots in the standard logit lens and exploring Belrose et al.’s augmentation of it.

Consider a Transformer with L layers, each operating in a latent space with dimensionality D . Denote the hidden state of the token used by the final prediction head after $0 \leq \ell \leq L$ hidden layers of the model have been processed as $h_{\text{out}}^{\ell+1} \in \mathbb{R}^D$.

The ℓ -th layer of the model performs the update,

$$h_{\text{out}}^{\ell+1} = h_{\text{out}}^\ell + F_\ell(h_{\text{out}}^{\ell+1}),$$

to this hidden state, where $F_\ell(\cdot)$ is the residual update of the ℓ -th layer.

Applying the residual update rule recursively, we observe that the final hidden state h_{out}^{L+1} is given by

$$h_{\text{out}}^{L+1} = h_{\text{out}}^\ell + \sum_{\ell'=\ell}^L F_{\ell'}(h_{\text{out}}^{\ell'+1}).$$

The calculation of the logit vector z^L can then be formalized as follows:

$$z^L = \text{LayerNorm} \left(h_{\text{out}}^\ell + \sum_{\ell'=\ell}^L F_{\ell'}(h_{\text{out}}^{\ell'+1}) \right) W_U + b_U.$$

Here, $\sigma(\cdot)$, W_U , and b_U denote the softmax function, unembedding matrix, and unembedding bias respectively.

The logit lens [36] computes the intermediate logit distribution before any layer ℓ , z^ℓ , by setting the residual update of future layers to zero:

$$z^\ell = \text{LayerNorm}(h_{\text{out}}^\ell) W_U + b_U.$$

Although this simple design works well for models such as GPT-2 [38], it fails to retain its effectiveness across model families [37]. Furthermore, the logit lens suffers from *bias* (it often places more probability mass on certain tokens than the prediction layer does) and *representation drift* (where the latent space of intermediate layers may not align with that of the final layer).

To correct for these flaws, the Tuned Lens introduces a learned translator composed of a weight matrix $A_\ell \in \mathbb{R}^{D \times D}$ and bias $b_\ell \in \mathbb{R}^D$ to the logit lens formulation, obtaining z_ℓ as follows:

$$z_\ell = \text{LayerNorm}(h_{\text{out}}^\ell A_\ell + b_\ell) W_U + b_U.$$

The two additions that the Tuned lens makes each account for a different shortfall of the original logit lens. The constant b_ℓ debiases the lens by learning the average residual update, thereby correcting for cases where the Transformer’s average updates significantly deviate from zero. The weights A_ℓ function as a change-of-basis matrix that maps the intermediate latent space to that used by the final layer. After training to minimize KL-divergence against prediction logits yielded from the original Transformer, the Tuned Lens yields substantially lower bias and perplexity than the standard logit lens.

In QLENS, we adopt the Tuned Lens as a foundation from which the model’s latent probabilities can be examined. We note that the space of possible probabilities is constrained, primarily by the condition that applying softmax to logits ensures that they are normalized to sum to 1. This motivates the translation of the mathematics of quantum mechanics: its definition of state vectors and unitary operators renders it uniquely suited to describe transformations between probability distributions. We formally introduce QLENS in the subsequent section.

4 The QLENS Framework

To make the relationship between Transformers and QM concrete, we now formally introduce QLENS’s postulates of a quantum-inspired perspective of Transformers. Please note that this section is not intended to be interpreted as a direct isomorphism between the two subjects, but rather as a simple framing of the internals of Transformers in the language of QM to motivate QLENS’s protocol design. The postulates of QLENS mirror the fundamental principles of quantum mechanics and provide definitions of Hilbert spaces, state vectors, unitary operators, Hamiltonians, and measurement operators in the context of Transformers. By deriving these quantities for trained Transformer, insights regarding the action of its layers may be obtained. An overview of our analogy is presented in Table 1.

Broadly, a state vector of a Transformer is a transformed representation of its internal probability distribution, whose expansion in the Hilbert basis reflects the component of the total probability mass afforded to each token. The model’s state vector is successively modified by the layers of a Transformer, which are treated as unitary operators learned during training. Extending this structure yields a Hamiltonian associated with each layer that serves as the generator of an analogous

Quantum Mechanics	QLENS Transformer Analog	QLENS Interpretation
Hilbert basis of states \mathcal{H}	Hilbert basis for tokens \mathcal{C}	Each basis vector corresponds to a distinct token, or state
State vector $ \Psi\rangle$	Model state vector $ \Psi^\ell\rangle$	The state vector encapsulates the model's probability distribution for predicted tokens at after the processing of ℓ layers
Unitary operator \mathbf{U}	Layer unitary operator \mathbf{U}^ℓ	Layers evolve state vectors in adherence to the Schrödinger equation, with their action governed by the weights learned in training
Hamiltonian \mathbf{H}	Layer Hamiltonian \mathbf{H}^ℓ	Eigenvectors and eigenvalues of layer Hamiltonian reflect the dynamics state vector evolution in layers
Measurement operator \mathbf{L}	Sampling operator \mathbf{M}	The sampling operator maps the final state vector to probabilities for each token

Table 1: An overview of the links between Transformers and QM formed by QLENS.

residual stream output. After passing through all hidden layers, the state vector is converted into a concrete probability distribution through a sampling operator. Together, these postulates provide a novel end-to-end perspective of Transformer dynamics. We discuss each independently below, followed by a side-by-side comparison of the unified QLENS framework and the standard Transformers architecture.

4.1 Postulate 1: Hilbert Basis

One of the most fundamental concepts in QM is the state space of a particle, formally categorized as a Hilbert space. In QM, each basis vector of this space specifies a distinct state of a particle, such as spin-up $|u\rangle$ or spin-down $|d\rangle$. Akin to a quantum system's confinement to a finite number of measurable outcomes, a Transformer is restricted to a delimited set of distinct outputs. For a Transformer, the group of unique possible outputs for a given input sequence is the set of output units $\mathcal{C} = \{c_1, c_2, c_3, \dots, c_N\}$, with N representing the number of possible outputs for the model. Accordingly, a natural basis for a Transformer is the set of vectors $\mathcal{C} = \{|c_1\rangle, |c_2\rangle, |c_3\rangle, \dots, |c_N\rangle\}$, where each basis vector $|c_i\rangle \in \mathbb{C}^N$ corresponds to the i -th token in the model's vocabulary.

4.2 Postulate 2: Orthogonality of Basis Vectors

QM delineates that unambiguously distinguishable states must be ascribed orthogonal vectors. As a Transformer cannot output two distinct output units at once, these states are discernible by the action of selecting from its probability distribution. Thus,

$$\langle c_i | c_j \rangle = \begin{cases} 0, & \text{for } i \neq j \\ 1, & \text{for } i = j \end{cases} \quad (1)$$

It is also conventional for Hilbert bases to be normal. This can be expressed mathematically as the condition:

$$\| |c_i\rangle \|^2 = 1. \quad (2)$$

To satisfy eqs. 1 and 2 in conjunction, we elect to express the i -th basis vector as the following column vector:

$$|c_i\rangle = \begin{pmatrix} x_1 \\ x_2 \\ \vdots \\ x_n \end{pmatrix} \quad \text{where } x_j = \delta_{ij},$$

where δ_{ij} refers to the Kronecker delta symbol. In other words:

$$|c_i\rangle = \begin{pmatrix} 0 \\ \vdots \\ 1 \\ \vdots \\ 0 \end{pmatrix} \leftarrow i\text{-th position.}$$

This form is similar to a one-hot encoding of each output unit and defines the basis \mathcal{C} as orthonormal. This insight will prove crucial in forthcoming derivations involving Transformer state vectors, which are introduced in the following postulate.

4.3 Postulate 3: State Vectors

In the domain of NLP, Transformers operate by iteratively transforming a sequence of token representations to produce an output state for each token which may be used for token-level or sequence-level predictions, depending on task specifics. Given an input token sequence of length n , $I = \{i_1, i_2, i_3, \dots, i_n\}$ such that $\forall i \in I, i \in T$, where $T = \{t_1, t_2, t_3, \dots, t_V\}$ is the model vocabulary of size V , a Transformer produces an over distribution θ all elements in \mathcal{C} . In the Hilbert basis \mathcal{C} , this distribution can be ascribed a corresponding state vector denoted as $|\Psi\rangle$. This stems from the standard quantum formulation, where the notion of a state vector is intimately tied to the probabilities distribution of outcomes that would be observed if a measurement were to be conducted. To emulate this principle, $|\Psi\rangle$ is defined such that

$$P(c_i) = \langle c_i | \Psi \rangle \langle \Psi | c_i \rangle = |\langle c_i | \Psi \rangle|^2, \quad (3)$$

where $P(c_i)$ is the probability that the output unit c_i is generated by the Transformer. If $h_{\text{out}} \in \mathbb{R}^D$ is the final hidden state (post layer norm) for the token used by the prediction head of a Transformer with a D -dimensional embedding space, then the logit vector over the entire vocabulary is obtained by a linear transformation of h_{out} . The probability $P(c_i)$ is then the i -th component of the probability distribution resulting from applying the softmax function to this logit vector:

$$P_{j+1}(c_i) = \sigma(h_{\text{out}} W_U + b_U)_i. \quad (4)$$

Here, $W_U \in \mathbb{R}^{D \times N}$ and $b_U \in \mathbb{R}^N$ are the unembedding matrix and bias of the Transformer, and $\sigma(\cdot)$ is the softmax function.

However, a similar process can also be executed after the completion of any intermediate layer in the model as well to track the evolution of its internal probability distribution during inference time [36, 4]. Consider a Transformer with L hidden layers. Let $h_{\text{out}}^\ell \in \mathbb{R}^D$ denote the hidden state of the token used by the prediction head after the outputs of ℓ layers in the model architecture have been added to the residual stream. For clarity, h_{out}^0 would be the hidden state post-embedding and positional encoding, h_{out}^L would be the final hidden state before unembedding. Then, likewise to eq. 3 above, the hidden state h_{out}^ℓ can be mapped to the model's vocabulary through a function $f : \mathbb{R}^D \rightarrow \mathbb{R}^V$. In practice, this function can take the form of the logit lens [36] or one of its enhanced variants [4]. Thus, matching the structure of eq. 4 above, the state vector $|\Psi^\ell\rangle$ for this token after the processing of t layers is given by solving

$$|\langle c_i | \Psi^\ell \rangle|^2 = P^\ell(c_i) = \sigma[f(h_{\text{out}}^\ell)]_i \quad (5)$$

over all units in the output space, with $P^\ell(c_i)$ referring to the probability of generating the unit c_i after ℓ layers. This implies that $|\Psi^\ell\rangle$ has the column form:

$$|\Psi^\ell\rangle = \begin{pmatrix} \sqrt{P^\ell(c_1)} \\ \sqrt{P^\ell(c_2)} \\ \vdots \\ \sqrt{P^\ell(c_N)} \end{pmatrix} \quad (6)$$

Intuitively, this means that the k -th component of the state vector has a magnitude given by the square root of the probability of obtaining the k -th unit in the model’s output space. A consequence of this is that

$$\|\Psi^\ell\| = \sqrt{\langle\Psi^\ell|\Psi^\ell\rangle} = 1, \quad (7)$$

which corresponds to the fact that summing probabilities over all tokens yields one. The ket $|\Psi^\ell\rangle$ is layer-dependent, and the mechanism for its evolution is introduced in the next postulate.

4.4 Postulate 4: Layers and Schrödinger Dynamics

The primary function of a Transformer layer is to nudge its inputs towards outputs that better reflect the correct frequency distribution for later tokens in the relevant context. Building on the framework described thus far, we can now examine how an Transformer’s internal state evolves during its forward pass. Employing the notation of eq. 7, the ℓ -th hidden layer of an Transformer can be characterized as mapping the input product state vector $|\Psi^{\ell-1}\rangle \rightarrow |\Psi^\ell\rangle$, the resulting output. In QM, such state transitions are governed by the Schrödinger equation and are facilitated by unitary operators. Therefore, in this analogy we devise a unitary operator $\mathbf{U}^\ell \in \mathbb{C}^{N \times N}$ to describe the action of the ℓ -th Transformer layer on its input state vector:

$$|\Psi^\ell\rangle = \mathbf{U}^\ell |\Psi^{\ell-1}\rangle \quad \forall \ell \in \mathbb{Z}, 1 \leq \ell \leq L. \quad (8)$$

For clarity, we highlight that the unitary operator \mathbf{U}^ℓ , and by extension the Hamiltonian \mathbf{H}^ℓ (defined in the following postulate), is dependent on the layer’s input. In general, a Transformer prediction trajectory will not be identical across dataset instances, and thus a single operator is unable to represent this complexity by itself. Instead of narrowing to one input, QLENS computes operators across a broad set of examples to analyze holistic patterns as illustrated in section 5.

As a technical note, quantum mechanical unitary operators are generally functions of time, whereas to translate this concept to Transformers we remove this time dependence by considering a fixed time interval, as in common in domains such as quantum computing [35]. By applying the operators corresponding to each hidden layer of a Transformer in succession, the composite state vector begins as $|\Psi^0\rangle$ and travels through the Hilbert space \mathcal{C} , gradually converging to its final state $|\Psi^L\rangle$.

We briefly remark that this process is similar to that behind quantum computing algorithms such as Grover’s algorithm [19], where a desired state vector is strategically manipulated by a combination of quantum gates to prepare a desired output distribution [35, 48].

4.5 Postulate 5: The Hamiltonian Lens

By framing Transformer layers as unitary operators, we obtain access to additional tools from QM to investigate their action on state vectors. Specifically, we can now associate each layer’s unitary \mathbf{U}^ℓ with a Hamiltonian \mathbf{H}^ℓ . We will now discuss the properties of this Hamiltonian, demonstrating its connection with the change in the merged state vector $|\Psi^\ell\rangle$ over a layer.

QM dictates that Hamiltonian generates its associated unitary in accordance with the following relation derived from solving the time-dependent Schrödinger equation [52]:

$$\mathbf{U}(t) = \exp\left(\frac{-it\mathbf{H}}{\hbar}\right).$$

In converting the above equation to our description of Transformers, we substitute $\mathbf{U}(t)$ and \mathbf{H} with our defined analogs of \mathbf{U}^ℓ and \mathbf{H}^ℓ . In this exchange, we also replace the quantity $\frac{t}{\hbar}$ with a coefficient α , which captures the relevant factors at play while generalizing beyond the constants of QM.

$$\mathbf{U}^\ell = \exp(-i\alpha\mathbf{H}^\ell). \quad (9)$$

As in QM, the unitary constraint on \mathbf{U}^ℓ configures \mathbf{H}^ℓ to be Hermitian. Therefore, the eigenvectors of \mathbf{H}^ℓ specify a valid basis to expand $|\Psi^\ell\rangle$. in:

$$|\Psi^\ell\rangle = \sum_j k_j |E_j^\ell\rangle \quad \text{s.t. } \mathbf{H}^\ell |E_j^\ell\rangle = E_j^\ell |E_j^\ell\rangle \quad \text{and } || |E_j^\ell\rangle || = 1 \quad (10)$$

Using eqs. 8, 9, and 10, we put forth the following theorem that illustrates that this Hamiltonian is intimately tied to the change in the model’s state vector over the course of a layer.

Theorem 1. *Given a state vector $|\Psi^\ell\rangle$ that passes through layer ℓ with unitary \mathbf{U}^ℓ , the change $|\Delta\Psi^\ell\rangle$ during this process is completely determined by the eigenvectors and eigenvalues of the Hamiltonian \mathbf{H}^ℓ . Specifically,*

$$|\Delta\Psi^\ell\rangle = \sum_j k_j (e^{-i\alpha E_j} - 1) |E_j^\ell\rangle.$$

Proof. Presented in Appendix A.1. □

Through Theorem 1, the residual addition of Transformers can now be viewed through the lens of the Hamiltonian. Just as a standard Transformer layer produces a residual output that is combined with the previous hidden state to form the input for the subsequent layer, the unitary formulation of QLENS is equivalent to updating the model’s state vector by an amount $|\Delta\Psi^\ell\rangle$ solely subject to the properties of the Hamiltonian. The eigenvalues of the Hamiltonian dictate the proportional change in the component of the state vector along each of the Hamiltonian’s eigenvectors through the term $(e^{-i\alpha E_j} - 1)$. Each E_j provides a phase angle for the modification of the state vector in a particular direction of the Hilbert space, and α acts as a general layer-specific scaling factor. Therefore, while the unitary description of layers suggests compositional multiplication of the model’s state vector, the Hamiltonian produces the same process through simple vector addition. By carrying out this process across all layers of a trained model, the state vector shifts to approximate the true distribution for the subsequent tokens. The process of extracting this distribution in the final layer of the model is presented in the following postulate.

4.6 Postulate 6: Measurement Operators

The derivation of an output distribution from an Transformer bears parallels with the action of measurement in QM. In QM, measurement operators quantify the expected frequency of each possible outcome of an observation by mapping state vectors to probability distributions. The inherent randomness of QM is echoed in the stochasticity of generative NLP Transformers (e.g. Large Language Models), where each output is sampled from an underlying distribution. It follows that an appropriate set of outcomes and a corresponding operator \mathbf{M} may be derived for the state vectors delineated in subsection 4.3.

We begin by formalizing possible outcomes in the context of Transformers. In QM, these outcomes are numerical values that specify the eigenvalues of their measurement operator. For Transformers, the set of valid output results is $R = \{1, 2, 3, \dots, N\}$, where each element $r \in R$ coincides with the output ID of an output unit c_r .

To construct \mathbf{M} , it is helpful to first describe the desired behavior of applying \mathbf{M} to our basis vectors. If the state $|\Psi^\ell\rangle$ is a basis vector $|c_i\rangle$, then it refers to a situation in which the probability of sampling the token c_i is one. In other words, $|c_i\rangle$ is the state where the result of sampling is guaranteed to be i . As i was previously established to be an eigenvalue of \mathbf{M} ($i \in R$), $|c_i\rangle$ must be its dual eigenvector. By the definition of eigenvalues and eigenvectors, \mathbf{M} obeys

$$\mathbf{M} |c_i\rangle = i |c_i\rangle \quad \forall |c_i\rangle \in \mathcal{C}. \quad (11)$$

This relation is sufficient to determine the matrix elements of \mathbf{M} . Each entry is given by:

$$m_{kj} = \langle c_k | \mathbf{M} |c_j\rangle.$$

Substituting eq. 11, we obtain

$$m_{kj} = \langle c_k | j |c_j\rangle = j \langle c_k | c_j\rangle.$$

Applying the orthogonality condition of eq. 1, we find that

$$m_{kj} = j \delta_{kj}, \quad (12)$$

where δ_{kj} is once again the Kronecker delta symbol. Equivalently,

$$\mathbf{M} = \begin{pmatrix} 1 & 0 & 0 & \cdots & 0 \\ 0 & 2 & 0 & \cdots & 0 \\ 0 & 0 & 3 & \cdots & 0 \\ \vdots & \vdots & \vdots & \ddots & \vdots \\ 0 & 0 & 0 & \cdots & N \end{pmatrix}. \quad (13)$$

Identical to the quantum case, \mathbf{M} is also Hermitian with $\mathbf{M} = \mathbf{M}^\dagger$. This matrix mathematically summarizes the action of extracting an output distribution from an Transformer and lays the groundwork for our analogy of its last layer. We cover this aspect of QLENS, along with its merger with the rest of our proposal, in depth in the subsequent section.

4.7 End-to-End QLENS Framework

In this subsection, we consolidate the elements of QLENS into an integrated interpretation of a forward pass through a Transformer. A comparison between the standard Transformer design and our quantum analogy of it is illustrated in figure 1. We adhere to its structure in this synopsis, demonstrating the compatibility of QLENS with the inputs and outputs of a Transformer while providing a novel perspective on the model’s intermediate operation.

Consider a pretrained Transformer with vocabulary of tokens $T = \{t_1, t_2, t_3, \dots, t_V\}$. When this model receives a prompt, it is tokenized into an input sequence $I_n = \{i_1, i_2, i_3, \dots, i_n\}$ in which $\forall i \in I, i \in T$. All input tokens are then converted to embedding vectors such that the j -th token in I_n is converted into an embedding vector $h_j^0 \in \mathbb{R}^D$. While these vectors serve as the direct input to a Transformer’s hidden layers in the traditional paradigm, in QLENS they are used to extract an initial state vector for the model’s predictions. Specifically, the initial hidden state of the prediction token h_{out}^0 is associated with a ket $|\Psi^0\rangle \in \mathcal{C}$, where $\mathcal{C} = \{c_1, c_2, c_3, \dots, c_N\}$ is the Hilbert basis of the output units for the model. The expansion of $|\Psi^0\rangle$ in \mathcal{C} is given by eq. 6, where each component is computed using the Tuned Lens in conjunction with eq. 5.

This model state is systematically refined by the model layers, recast as unitary operators in QLENS. The ℓ -th hidden layer, governed by unitary \mathbf{U}^ℓ , intakes state $|\Psi^{\ell-1}\rangle$ and evolves it into $|\Psi^\ell\rangle$. The state vector $|\Psi^\ell\rangle$ aligns with the original Transformer’s residual stream after layer ℓ . Additional insights into the workings of the ℓ -th layer are derived by extracting its Hamiltonian \mathbf{H}^ℓ and analyzing its eigenvalues and eigenvectors. The eigenvectors specify the directions within \mathcal{C} that $|\Psi^\ell\rangle$ experiences a change, while the corresponding eigenvalues quantify the proportional extent of this change. Through the Hamiltonian, the change $|\Delta\Psi^\ell\rangle$ can be computed and functions as an analog of the residual output of the layer ℓ .

After navigating through all unitary operators, the hidden layers culminate in the production of the state $|\Psi^L\rangle$ containing the tuned probability distribution for the token that logically follows from the input sequence. The output probability distribution is found by computing the analogous Born rule:

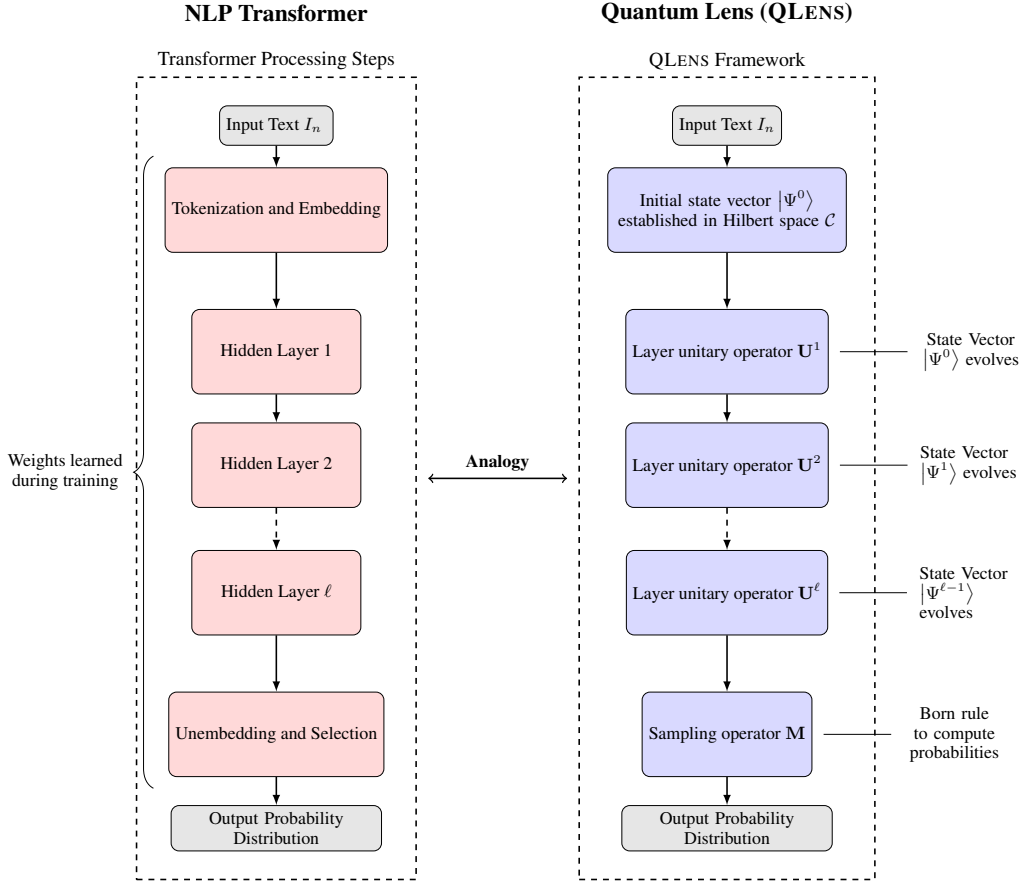


Figure 1: A side-by-side comparison of the standard architecture for an NLP Transformer and the QLENS framework.

$$P(i) = \langle c_i | \Psi^L \rangle \langle \Psi^L | c_i \rangle = |\langle c_i | \Psi^L \rangle|^2, \quad (14)$$

where i and $|c_i\rangle$ are the eigenvalues and eigenvectors of the sampling operator \mathbf{M} . An output unit is then selected according to this distribution using a decoding algorithm of choice.

With this guiding conceptualization, analogs of state vectors, unitary operators, and Hamiltonians can be procured from a pretrained model. Analyzing these quantities can provide insights into the general action of layers (e.g. do some layers tend to favor concentrating probability on one output unit over another), thus providing a perspective on the sequential change in model predictions during inference. To show how this analogy translates into an application, we draw inferences about the layers in a toy-model Transformer as a proof-of-concept in the ensuing section.

5 Experiments

We now operationalize QLENS by extracting state vectors, unitary operators, and Hamiltonians from a simple NLP Transformer on a sentiment classification task. We describe our experimental setup, followed by our results and interpretations of them.

5.1 Experimental Setup

We train a Transformer toy model on the *Sentihood* dataset [44] to perform QLENS analysis on. Sentihood is set of 5212 annotated sentences taken from Yahoo! Answers posts reviewing urban neighborhoods in London. Each instance is labeled with one or more *aspects*—specific character-

istics of the location(s) mentioned in the accompanying sentence (e.g., transportation availability, safety). For each aspect, Sentihood includes the reference target location in the sentence and the sentiment (positive or negative) expressed towards that aspect.

To simplify this dataset for the purposes of this toy-model, we preprocess the dataset by removing all instances involving multiple locations or aspects. In doing so, we retain only the features of the sentence text and the sentiment associated with it. This leaves 1,864 instances, of which 1,329 convey positive sentiment and 535 indicate negative sentiment. We further balance the dataset to an exact 1:1 ratio of positive and negative sentiment instances, yielding a final corpus of 1,070 instances (535 positive and 535 negative). This corpus is then divided into train and test sets with in accordance to an 80:20 ratio.

On this preprocessed dataset, we train a simple Transformer model with a single decoder block to classify the sentiment of input texts to the model. Sentence tokenization and embedding is conducted by using the GPT-2 [38] tokenizer (extended to prepend a classification token to each instance) and its embedding and positional encoding matrices, producing 768-dimensional embeddings. Due to computational limitations, we compress these embeddings to a dimensionality of 12 via a learnable linear layer before passing through the remainder of the model. These embeddings are then updated by a four-headed attention layer [50] before passing through a feed-forward network, which uses the ReLU activation function and has an intermediate dimensionality of 48. Both the attention and feed-forward layers include post-layer normalization. The layer-normalized hidden state of the MLP layer is subsequently mapped to logits through a linear classification layer and softmax-normalized to obtain class probabilities. We train this Transformer for 12 epochs using binary cross-entropy loss against the sentiment labels, resulting in a test accuracy of 0.7944.

Upon this Transformer, we train two separate tuned lenses to derive intermediate probability distributions from the model. These lenses are instantiated as bias-only lenses without the translator weight matrix A_ℓ due to the simplicity of our toy model. The *embedding lens* is trained using the hidden states produced by the Transformer after the initial GPT-2 embeddings are compressed. Similarly, the *attention lens* is conditioned upon the post-attention hidden states. These two lenses, combined with the output probability distribution produced by the model, allow us to track model prediction trajectories at three distinct stages in its inference.

Specifically, for each instance in the preprocessed dataset, we compute the three aforementioned probability distributions and use them to extract three state vectors (eqs. 5 and 6), denoted $|\Psi^0\rangle$, $|\Psi^1\rangle$, and $|\Psi^2\rangle$ in accordance with our previously established notation. We then construct appropriate unitary operators U^1 and U^2 to map between states $|\Psi^0\rangle$ and $|\Psi^1\rangle$ and states $|\Psi^1\rangle$ and $|\Psi^2\rangle$ respectively (eq. 8). Consequently, the operator U^1 describes the action of the attention layer, while correspondingly U^2 illuminates that of the feed-forward layer. We note that in general there exist an infinite number of possible unitary matrices that map from one state to another, and thus choose to constrain the form of the operators U^1 and U^2 to be Householder transformations [23] for their practical efficiency and simplicity. These transformations can be viewed as reflections across a reflection plane, given by

$$I - 2|v\rangle\langle v|,$$

where $|v\rangle$ is the normal vector for the reflecting hyperplane. Alongside these unitary operators, we derive their associated Hamiltonians (eq. 9). These Hamiltonians provide a quantum-mechanical representation of residual updates, enabling QLENS to cohesively compute the changes of the state vector between layers. To validate this approach, we put QLENS into practice by analyzing the empirical data produced by it and presenting our interpretation.

5.2 Results and Analysis

To search for trends in the action of the multi-head attention and MLP layers with QLENS, we examine the distribution of pairwise Frobenius cosine similarities between unitary operators extracted from dataset instances. Both the attention and MLP layers exhibit higher mean pairwise similarities between unitary operators than those of the randomly initialized control (Table 2). We evaluate the statistical significance of these differences by conducting two-sample permutation tests for each layer with the alternative hypothesis that the intra-layer unitary operator similarity is greater than then control. The unitary operators derived from each layer were pooled with those of the baseline before being randomly split into two groups whose intra-group similarity metrics were compared

Layer	Mean Pairwise Unitary Operator Frobenius Similarity (Baseline: 0.00)	P value of Mean Pairwise Unitary Operator Frobenius Similarity	Mean Pairwise Hamiltonian Frobenius Similarity (Baseline: 0.50)	P value of Mean Pairwise Hamiltonian Frobenius Similarity	Average $ \Delta\Psi\rangle$
Multi-headed Attention	0.8398	0.0001	0.9193	0.0001	$\begin{pmatrix} -0.1001 \\ -0.0385 \end{pmatrix}$
Multi-Layer Perceptron	0.4901	0.0001	0.7445	0.0001	$\begin{pmatrix} -0.0009 \\ 0.0003 \end{pmatrix}$

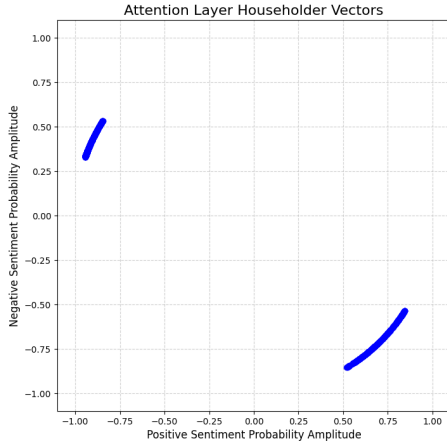
Table 2: A summary of the numerical results derived by QLENS for a simple sentiment classification Transformer.

against the observed values. We simulate 1,000 permutations and apply add-one smoothing to account for finite approximation error. Finding no instances where a randomized group resulted in higher similarity than observed, we obtain a p value of approximately 0.0001 in both cases. This suggests that while each layer modifies unique inputs in distinct ways, the transformations enacted by them demonstrate an overall consistency.

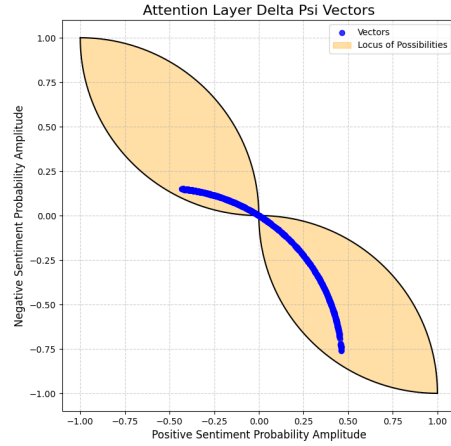
Furthermore, we test the mean pairwise similarity of the Hamiltonians of both layers in order to probe these structural regularities in greater depth. This separate analysis helps confirm whether the consistency observed in the transformations \mathbf{U}^ℓ are rooted in a consistent generator of change \mathbf{H}^ℓ across different inputs. For both attention and MLP, these Hamiltonian demonstrate higher intra-layer similarity than in their corresponding unitary operators, a finding that can be partially attributed to the increase in the randomized control Hamiltonian similarities over those for unitaries. Nevertheless, permutation tests designed analogously to those for unitary operations likewise produce p values of 0.0001 (Table 2), signaling that there is convincing statistical evidence that these similarities in Hamiltonians remain significantly greater than the randomized baseline.

We further shed light on these similarities by creating a scatter plot of the normalized Householder vectors characterizing them. For the attention layer, these vectors form two concentrated clusters within sparse angular intervals (Figure 2a). Due to the structure of their definition in eq. 6, model state vectors occupy quadrant I. Consequently, the space of all normal vectors of the Householder reflection plane is the union of arcs of the unit circle in quadrants II and IV. Thus, this dense clustering suggests that not all probability updates are realized by the attention layer; rather, it relies on a constrained portion of all valid updates in its prediction trajectory. To evaluate this hypothesis, we turn to the associated Hamiltonians of the attention layer. Through them, we employ Theorem 1 to extract state vector changes across the attention layer and graph the results on a separate scatter plot (Figure 2b). In alignment with previous results, while the locus of all possible changes in state vectors is the region in yellow (see Appendix A2 for proof), all vectors lie on a limited arc. Intriguingly, this arc is not symmetric in quadrants II and IV, rather there is a nonzero average change in state vector that lies in quadrant II. This implies that this attention layer is biased—it tends to increase the probability mass of positive sentiment over negative sentiment.

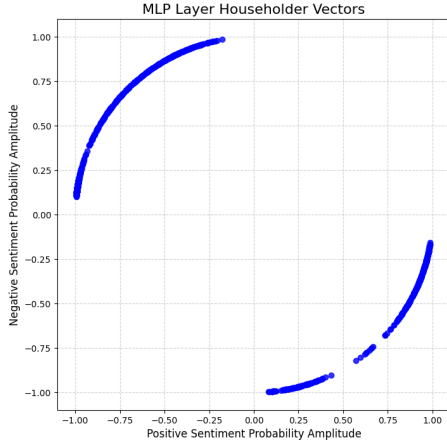
Conducting a similar analysis on the MLP layer, we find a greater spread in its Householder vectors (Figure 2c). This variance explains the relatively lower similarity of both unitary operators and Hamiltonians in the MLP layer, as these quantum quantities are mathematically linked to the Householder vector. Accordingly, the MLP may be capable of realizing a wider variety of probability updates and state transformations than the attention layer. However, the plot of state vector changes modifies this deduction, as all vectors cluster tightly around the origin (Figure 2d). Therefore, the MLP layer modifies state vectors along a more diverse collection of directions than the attention layer, but contributes significantly less to the Transformer’s final predictions, making only minute refinements instead. This finding is in agreement with previous literature that has revealed that earlier layers in a Transformer have a larger impact on downstream outcomes [45]. However, whereas these works compare prediction accuracy metrics of models with selectively removed lay-



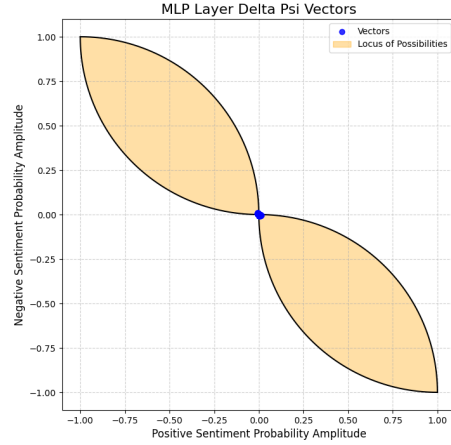
(a) Attention Layer Householder vectors



(b) Attention Layer $|\Delta\Psi\rangle$



(c) MLP Layer Householder vectors



(d) MLP Layer $|\Delta\Psi\rangle$

Figure 2: A collection of visualizations produced by the QLENS method on a sentiment classification Transformer. For each layer in the model (attention and MLP), two key components are illustrated: the Householder vectors of its derived unitary operators and the change in the model’s state vector across it.

ers, QLENS supplies a fine-grained and mechanistic method to track each layer’s influence through the mathematics of QM.

6 Limitations and Open Research Directions

The formulation of QLENS provides a novel framework for interpreting Transformers from the perspective of quantum mechanics. However, as is common with interdisciplinary work, the current perspective raises multiple intriguing challenges and open questions that warrant future investigation. We acknowledge these considerations here to guide future research in this area.

A significant difference between QM and Transformers is that QM and its associated operators are structurally linear [49], whereas Transformers derive many of their capabilities from their nonlinear components and activation functions [2, 8, 21, 40]. This challenge of nonlinearities has been previ-

ously observed in work on quantum machine learning algorithms [32]. In this paper, we reconcile these distinctions by conducting our initial analysis with QLENS at a level of abstraction above the underlying processes inside Transformer layers, instead modeling them primarily as input-to-output functions. Nevertheless, comprehensively conquering the nonlinearities involved and expanding QLENS to model the intra-layer processes of MLPs and Attention blocks remain open challenges.

Furthermore, we note that the experimental inferences that emerged from the proof of concept of QLENS may not generalize to other Transformers due to the limited scope of our initial experiments. However, the technique introduced by QLENS is flexible, allowing it to be extended to pretrained NLP Transformers across scales and task specifics. We intend to continue to explore this area with future supplemental studies on the capabilities of QLENS.

Taking into consideration these current gaps and opportunities, we present this paper as an initial result exploring the potential parallels between these two domains. We hope that the mathematical language and method introduced in this work lay the groundwork for future studies to build more cohesive theoretical ties between Transformers and QM that lead to a unique understanding of the former domain.

7 Conclusion

In this paper, we introduce QLENS, a framework that charts a new path towards a quantum-inspired perspective of Transformers. By identifying conceptual similarities between QM and transformers, we developed a set of analogs for the core postulates of quantum mechanics and employed them to recast the standard forward pass through a language Transformer. Specifically, we exhibit that latent activations, hidden layers, and the unembedding process can be formally mapped to state vectors, unitary operators, and a measurement operator, respectively, to replicate the probabilistic nature of Transformer through a proof-of-concept demonstration. This contribution opens several promising research directions for a quantum-based theoretical understanding of Transformers. Our work could be extended to integrate further components of quantum mechanics into this formalization, including entanglement to explore associations between layers and the general uncertainty principle for describing inherent inference tradeoffs, among others. A particularly noteworthy consequence of this research is the possibility to explore whether these analogies could be used to create new metrics for interpreting and evaluating Transformers. For instance, studies could adapt quantum information-theoretic measures to gauge the influence of model hidden states from previous layers on future ones, offering an alternative viewpoint on contextual dependence in Transformer inference. Furthermore, our work can function as a basis to examine whether such parallels hint at a deeper physical structure underpinning Transformers. We intend to continue to explore this area by scaling the implementation of QLENS to larger model sizes and investigating methods to address the critical nonlinearities in Transformers through the lenses of quantum channels and nonlinear Schrödinger equations.

References

- [1] David H. Ackley and Geoffery E. Hinton. A learning algorithm for boltzmann machines. *Cognitive science*, 9(8):147–169, 1985.
- [2] Abien Fred Agarap. Deep learning using rectified linear units (relu). *ArXiv*, abs/1803.08375, 2018.
- [3] Jimmy Ba, Jamie Ryan Kiros, and Geoffrey E. Hinton. Layer normalization. *ArXiv*, abs/1607.06450, 2016.
- [4] Nora Belrose, Zach Furman, Logan Smith, Danny Halawi, Igor V. Ostrovsky, Lev McKinney, Stella Biderman, and Jacob Steinhardt. Eliciting latent predictions from transformers with the tuned lens. *ArXiv*, abs/2303.08112, 2023.
- [5] Alessandro Betti and Marco Gori. The principle of least cognitive action. *Theoretical Computer Science*, 633:83–99, 2016. Biologically Inspired Processes in Neural Computation.
- [6] Luis J. Boya. The thermal radiation formula of planck (1900). *ArXiv*, abs/physics/0402064, 2004.

- [7] Trenton Bricken, Adly Templeton, Joshua Batson, Brian Chen, Adam Jermyn, Tom Conerly, Nicholas L Turner, Cem Anil, Carson Denison, Amanda Askill, Robert Lasenby, Yifan Wu, Shauna Kravec, Nicholas Schiefer, Tim Maxwell, Nicholas Joseph, Alex Tamkin, Karina Nguyen, Brayden McLean, Josiah E Burke, Tristan Hume, Shan Carter, Tom Henighan, and Chris Olah. Towards monosemanticity: Decomposing language models with dictionary learning. 2023.
- [8] John S Bridle. Training stochastic model recognition algorithms as networks can lead to maximum mutual information estimation of parameters. In D. Touretzky, editor, *Advances in Neural Information Processing Systems*, volume 2. Morgan-Kaufmann, 1989.
- [9] Tom B. Brown, Benjamin Mann, Nick Ryder, Melanie Subbiah, Jared Kaplan, Prafulla Dhariwal, Arvind Neelakantan, Pranav Shyam, Girish Sastry, Amanda Askill, Sandhini Agarwal, Ariel Herbert-Voss, Gretchen Krueger, T. J. Henighan, Rewon Child, Aditya Ramesh, Daniel M. Ziegler, Jeff Wu, Clemens Winter, Christopher Hesse, Mark Chen, Eric Sigler, Ma teusz Litwin, Scott Gray, Benjamin Chess, Jack Clark, Christopher Berner, Sam McCandlish, Alec Radford, Ilya Sutskever, and Dario Amodei. Language models are few-shot learners. *ArXiv*, abs/2005.14165, 2020.
- [10] Diogo Vieira Carvalho, Eduardo Marques Pereira, and Jaime S. Cardoso. Machine learning interpretability: A survey on methods and metrics. *Electronics*, 2019.
- [11] Fu Chen, Qinglin Zhao, Li Feng, Chuangtao Chen, Yangbin Lin, and Jianhong Lin. Quantum mixed-state self-attention network. *Neural Networks*, 185:107123, 2025.
- [12] El Amine Cherrat, Iordanis Kerenidis, Natansh Mathur, Jonas Landman, Martin Strahm, and Yun Yvonna Li. Quantum Vision Transformers. *Quantum*, 8:1265, 2024.
- [13] Arthur Conmy, Augustine Mavor-Parker, Aengus Lynch, Stefan Heimersheim, and Adrià Garriga-Alonso. Towards automated circuit discovery for mechanistic interpretability. In A. Oh, T. Naumann, A. Globerson, K. Saenko, M. Hardt, and S. Levine, editors, *Advances in Neural Information Processing Systems*, volume 36, pages 16318–16352. Curran Associates, Inc., 2023.
- [14] Fahim Dalvi, Nadir Durrani, Hassan Sajjad, Yonatan Belinkov, Anthony Bau, and James R. Glass. What is one grain of sand in the desert? analyzing individual neurons in deep nlp models. In *AAAI Conference on Artificial Intelligence*, 2018.
- [15] Anna Dawid, Julian Arnold, Borja Requena, Alexander Gresch, Marcin Plodzie’ n, Kaelan Donatella, Kim Andrea Nicoli, Paolo Stornati, Rouven Koch, Miriam Buttner, Robert Okuła, Gorka Muñoz-Gil, Rodrigo A. Vargas-Hern’andez, Alba Cervera-Lierta, Juan Felipe Carrasquilla, Vedran Dunjko, Marylou Gabri’e, Patrick Huembeli, Evert van Nieuwenburg, Filippo Vicentini, Lei Wang, Sebastian Johann Wetzels, Giuseppe Carleo, Elivska Greplov’a, Roman V. Krems, Florian Marquardt, Michał Tomza, Maciej Lewenstein, and Alexandre Dauphin. Modern applications of machine learning in quantum sciences. *ArXiv*, 2022.
- [16] Jacob Devlin, Ming-Wei Chang, Kenton Lee, and Kristina Toutanova. Bert: Pre-training of deep bidirectional transformers for language understanding. In *North American Chapter of the Association for Computational Linguistics*, 2019.
- [17] Abhimanyu Dubey, Abhinav Jauhri, Abhinav Pandey, Abhishek Kadian, Ahmad Al-Dahle, Aiesha Letman, Akhil Mathur, Alan Schelten, Amy Yang, Angela Fan, Anirudh Goyal, Anthony S. Hartshorn, Aobo Yang, Archi Mitra, Archie Sravankumar, et al. The llama 3 herd of models. *ArXiv*, abs/2407.21783, 2024.
- [18] Adrian Erasmus, Tyler D. P. Brunet, and Eyal Fisher. What is interpretability? *Philosophy & Technology*, 34:833 – 862, 2020.
- [19] Lov K. Grover. A fast quantum mechanical algorithm for database search. In *Symposium on the Theory of Computing*, 1996.
- [20] Kaiming He, X. Zhang, Shaoqing Ren, and Jian Sun. Deep residual learning for image recognition. *2016 IEEE Conference on Computer Vision and Pattern Recognition (CVPR)*, pages 770–778, 2015.

- [21] Dan Hendrycks and Kevin Gimpel. Gaussian error linear units (gelus). *arXiv: Learning*, 2016.
- [22] J. J. Hopfield. Neural networks and physical systems with emergent collective computational abilities. *Proceedings of the National Academy of Sciences*, 79(8):2554–2558, 1982.
- [23] Alston S. Householder. Unitary triangularization of a nonsymmetric matrix. *J. ACM*, 5(4):339–342, October 1958.
- [24] Stanisław Jastrzebski, Devansh Arpit, Nicolas Ballas, Vikas Verma, Tong Che, and Yoshua Bengio. Residual connections encourage iterative inference. In *International Conference on Learning Representations*, 2018.
- [25] Ganesh Jawahar, Benoît Sagot, and Djamé Seddah. What does BERT learn about the structure of language? In Anna Korhonen, David Traum, and Lluís Màrquez, editors, *Proceedings of the 57th Annual Meeting of the Association for Computational Linguistics*, pages 3651–3657, Florence, Italy, July 2019. Association for Computational Linguistics.
- [26] J.H.O.Sales, A.T. Suzuki, and D.S. Bonafé. Revisiting bohr’s quantization hypothesis for the atomic orbitals. *ArXiv*, abs/physics/0608102, 2006.
- [27] Licheng Jiao, Xue Song, Chao You, Xu Liu, Lingling Li, Puhua Chen, Xu Tang, Zhixi Feng, Fang Liu, Yuwei Guo, Shuyuan Yang, Yangyang Li, Xiangrong Zhang, Wenping Ma, Shuang Wang, Jing Bai, and Biao Hou. Ai meets physics: a comprehensive survey. *Artif. Intell. Rev.*, 57(9):256, September 2024.
- [28] Sunwoo Kim, Haneul Yoo, and Alice Oh. On the effect of uncertainty on layer-wise inference dynamics. *ArXiv*, abs/2507.06722, 2025.
- [29] Xiaofei Kong, Lei Li, Meng-Han Dou, Zhaoyun Chen, Yuchun Wu, and Guoping Guo. Quantum-enhanced llm efficient fine tuning. *ArXiv*, abs/2503.12790, 2025.
- [30] Vedang Lad, Wes Gurnee, and Max Tegmark. The remarkable robustness of LLMs: Stages of inference? In *ICML 2024 Workshop on Mechanistic Interpretability*, 2024.
- [31] Hannah Lange, Guillaume Bornet, Gabriel Emperauger, Cheng Chen, Thierry Lahaye, Stefan Kienle, Antoine Browaeys, and Annabelle Bohrdt. Transformer neural networks and quantum simulators: a hybrid approach for simulating strongly correlated systems. *Quantum*, 9:1675, 2024.
- [32] Guangxi Li, Xuanqiang Zhao, and Xin Wang. Quantum self-attention neural networks for text classification. *Sci. China Inf. Sci.*, 67, 2022.
- [33] Ziming Liu, Yizhou Liu, Jeff Gore, and Max Tegmark. Neural thermodynamic laws for large language model training. *ArXiv*, abs/2505.10559, 2025.
- [34] Tomas Mikolov, Kai Chen, Gregory S. Corrado, and Jeffrey Dean. Efficient estimation of word representations in vector space. In *International Conference on Learning Representations*, 2013.
- [35] Michael A. Nielsen and Isaac L. Chuang. *Quantum Computation and Quantum Information*. Cambridge University Press, 2000.
- [36] nostalgebraist. Interpreting gpt: the logit lens.
- [37] nostalgebraist. logit lens on non-gpt2 models + extensions, 2021.
- [38] Alec Radford, Jeff Wu, Rewon Child, David Luan, Dario Amodei, and Ilya Sutskever. Language models are unsupervised multitask learners. 2019.
- [39] Daking Rai and Ziyu Yao. An investigation of neuron activation as a unified lens to explain chain-of-thought eliciting arithmetic reasoning of llms. In *Annual Meeting of the Association for Computational Linguistics*, 2024.
- [40] Prajit Ramachandran, Barret Zoph, and Quoc V. Le. Swish: a self-gated activation function. *arXiv: Neural and Evolutionary Computing*, 2017.

- [41] Hubert Ramsauer, Bernhard Schaffl, Johannes Lehner, Philipp Seidl, Michael Widrich, Lukas Gruber, Markus Holzleitner, Milena Pavlović, Geir Kjetil Ferkingstad Sandve, Victor Greiff, David P. Kreil, Michael Kopp, Günter Klambauer, Johannes Brandstetter, and Sepp Hochreiter. Hopfield networks is all you need. *ArXiv*, abs/2008.02217, 2020.
- [42] Frank Rosenblatt. The perceptron: a probabilistic model for information storage and organization in the brain. *Psychological review*, 65 6:386–408, 1958.
- [43] Sebastian Ruder. An overview of gradient descent optimization algorithms. *ArXiv*, abs/1609.04747, 2016.
- [44] Marzieh Saeidi, Guillaume Bouchard, Maria Liakata, and Sebastian Riedel. SentiHood: Targeted aspect based sentiment analysis dataset for urban neighbourhoods. In Yuji Matsumoto and Rashmi Prasad, editors, *Proceedings of COLING 2016, the 26th International Conference on Computational Linguistics: Technical Papers*, pages 1546–1556, Osaka, Japan, December 2016. The COLING 2016 Organizing Committee.
- [45] Hassan Sajjad, Fahim Dalvi, Nadir Durrani, and Preslav Nakov. On the effect of dropping layers of pre-trained transformer models. *Comput. Speech Lang.*, 77:101429, 2020.
- [46] Grant Sanderson. Attention in transformers, step-by-step — Deep Learning Chapter 6. YouTube, 2024. Video.
- [47] Grant Sanderson. How might LLMs store facts — Deep Learning Chapter 7. YouTube, 2024. Video.
- [48] Grant Sanderson. But what is quantum computing? (Grover’s Algorithm). YouTube, 2025. Video.
- [49] Leonard Susskind and Art Friedman. *Quantum Mechanics: The Theoretical Minimum*. Basic Books, New York, 2013.
- [50] Ashish Vaswani, Noam M. Shazeer, Niki Parmar, Jakob Uszkoreit, Llion Jones, Aidan N. Gomez, Lukasz Kaiser, and Illia Polosukhin. Attention is all you need. In *Neural Information Processing Systems*, 2017.
- [51] H.C. Verma. *Quantum Physics*. Surya Publications, 2009.
- [52] Colin P. Williams and Scott H. Clearwater. *Explorations in Quantum Computing*. Springer-Verlag TELOS, Santa Clara, CA, USA, 1997.
- [53] Yuanhua Zhang and Massimiliano Di Ventra. Transformer quantum state: A multipurpose model for quantum many-body problems. *Physical Review B*, 2022.
- [54] Haiyan Zhao, Hanjie Chen, F. Yang, Ninghao Liu, Huiqi Deng, Hengyi Cai, Shuaiqiang Wang, Dawei Yin, and Mengnan Du. Explainability for large language models: A survey. *ACM Transactions on Intelligent Systems and Technology*, 15:1 – 38, 2023.

A Appendix

A.1 Proof of Theorem 1: Deriving Changes in State Vectors from Hamiltonians

Proof. The change $|\Delta\Psi^\ell\rangle$ can be written in terms of input and output state vectors of the layer ℓ :

$$|\Delta\Psi^\ell\rangle = |\Psi^{\ell+1}\rangle - |\Psi^\ell\rangle.$$

Using eq. 8 we rewrite $|\Psi^{\ell+1}\rangle$ in terms of $|\Psi^\ell\rangle$:

$$|\Delta\Psi^\ell\rangle = \mathbf{U}^\ell |\Psi^\ell\rangle - |\Psi^\ell\rangle.$$

Substituting the results of eqs. 9 and 10 we find:

$$|\Delta\Psi^\ell\rangle = \left[\exp(-i\alpha\mathbf{H}^\ell) \sum_j k_j |E_j^\ell\rangle \right] - \sum_j k_j |E_j^\ell\rangle.$$

Applying the Taylor series expansion of the matrix exponential and reorganizing the summations we obtain:

$$|\Delta\Psi^\ell\rangle = \left[\sum_{m=0}^{\infty} \sum_j \frac{(-i\alpha\mathbf{H}^\ell)^m}{m!} k_j |E_j^\ell\rangle \right] - \sum_j c_j |E_j^\ell\rangle.$$

Since $|E_j^\ell\rangle$ is an eigenvector of \mathbf{H}^ℓ , we have $(\mathbf{H}^\ell)^m |E_j^\ell\rangle = (E_j)^\ell |E_j^\ell\rangle$. This allows us to put the above equation in the following form:

$$|\Delta\Psi^\ell\rangle = \left[\sum_{m=0}^{\infty} \sum_j \frac{(-i\alpha E_j)^\ell}{m!} k_j |E_j^\ell\rangle \right] - \sum_j k_j |E_j^\ell\rangle.$$

We now recondense the first summation by applying the earlier Taylor series relationship in reverse:

$$|\Delta\Psi^\ell\rangle = \sum_j k_j e^{-i\alpha E_j} |E_j^\ell\rangle - \sum_j k_j |E_j^\ell\rangle.$$

Factoring the right side of the expression into a simpler form, we procure a simplified equation for $|\Delta\Psi^\ell\rangle$:

$$|\Delta\Psi^\ell\rangle = \sum_j k_j (e^{-i\alpha E_j} - 1) |E_j^\ell\rangle.$$

This satisfies the conclusion of the theorem and we are done. \square

A.2 The Locus of State Vectors Updates

We begin with observation that the postulate that establishes state vectors for Transformers constrains them to possess only positive real components in \mathcal{C} . In particular, by eq. 6, any state vector $|\Psi^\ell\rangle$ lies on the surface of the unit N -dimensional hypersphere in the positive octant. The k -th component of $|\Psi^\ell\rangle$, $|\Psi^\ell\rangle_k$, is given by

$$|\Psi^\ell\rangle_k = \begin{cases} \cos(\theta_k) \prod_{i=1}^{k-1} \sin(\theta_i) & \text{if } 1 \leq k \leq N-1 \\ \prod_{i=1}^{N-1} \sin(\theta_i) & \text{if } k = N \end{cases}$$

where $\theta_1, \theta_2, \theta_3, \dots, \theta_N \in [0, \frac{\pi}{2}]$. Similarly, the updated state vector produced by the ℓ -th layer, $|\Psi^{\ell+1}\rangle$ can be parameterized by $\phi_1, \phi_2, \phi_3, \dots, \phi_N \in [0, \frac{\pi}{2}]$:

$$|\Psi^{\ell+1}\rangle_k = \begin{cases} \cos(\phi_k) \prod_{i=1}^{k-1} \sin(\phi_i) & \text{if } 1 \leq k \leq N-1 \\ \prod_{i=1}^{N-1} \sin(\phi_i) & \text{if } k = N \end{cases}$$

Thus, a vector $|\Delta\Psi^\ell\rangle$ is an element of the locus of difference vectors \mathcal{S} if it satisfies the relation $|\Delta\Psi^\ell\rangle = |\Psi^{\ell+1}\rangle - |\Psi^\ell\rangle$, or its more descriptive equivalent:

$$|\Delta\Psi^\ell\rangle_k = \begin{cases} \cos(\phi_k) \prod_{i=1}^{k-1} \sin(\phi_i) - \cos(\theta_k) \prod_{i=1}^{k-1} \sin(\theta_i) & \text{if } 1 \leq k \leq N-1 \\ \prod_{i=1}^{N-1} \sin(\phi_i) - \prod_{i=1}^{N-1} \sin(\theta_i) & \text{if } k = N \end{cases},$$

where each $\theta_i, \phi_i \in [0, \frac{\pi}{2}]$. For the case where $N = 2$, as in our toy model, the restriction on $|\Delta\Psi^\ell\rangle_k$ reduces to

$$|\Delta\Psi^\ell\rangle_k = \begin{cases} \cos(\phi) - \cos(\theta) & \text{if } k = 1 \\ \sin(\phi) - \sin(\theta) & \text{if } k = 2 \end{cases}$$

Rewriting $|\Delta\Psi^\ell\rangle$ in column form and applying the sum-to-product trigonometric identities we obtain:

$$|\Delta\Psi^\ell\rangle = \begin{pmatrix} -2 \sin\left(\frac{\phi-\theta}{2}\right) \sin\left(\frac{\phi+\theta}{2}\right) \\ 2 \sin\left(\frac{\phi-\theta}{2}\right) \cos\left(\frac{\phi+\theta}{2}\right) \end{pmatrix}.$$

We define $\delta = \phi - \theta$ and $\epsilon = \phi + \theta$ and simplify:

$$|\Delta\Psi^\ell\rangle = 2 \sin\left(\frac{\delta}{2}\right) \begin{pmatrix} -\sin\left(\frac{\epsilon}{2}\right) \\ \cos\left(\frac{\epsilon}{2}\right) \end{pmatrix} \quad \text{where } \delta \in \left[-\frac{\pi}{2}, \frac{\pi}{2}\right] \text{ and } \epsilon \in [0, \pi]$$

While this is a complete mathematical description of the elements of \mathcal{S} , a more intuitive understanding can be acquired by examining extreme cases. Consider fixing $\theta = 0$ while allowing δ to vary. This yields the arc

$$\begin{pmatrix} \cos(\phi) - 1 \\ \sin(\phi) - \sin(\theta) \end{pmatrix}$$

which is equivalent to the quarter circle traced by the graph of $(x+1)^2 + y^2 = 1$ from $(0, 0)$ to $(-1, 1)$. Likewise, if we fix $\phi = \frac{\pi}{2}$, then we obtain the arc formed by $x^2 + (y-1)^2 = 1$ between the same two points. These two quarter-circles bound the locus \mathcal{S} in quadrant II; the intersection of these disks is a \mathcal{R} comprising half of \mathcal{S} , with

$$\mathcal{R} = \{(a, b) : (a+1)^2 + b^2 \leq 1 \text{ and } a^2 + (b+1)^2 \leq 1\}.$$

Continuing this process by separately fixing $\theta = \frac{\pi}{2}$ and $\phi = 0$ yields a similar lobe \mathcal{T} in quadrant IV, given by:

$$\mathcal{T} = \{(a, b) : (a-1)^2 + b^2 \leq 1 \text{ and } a^2 + (b-1)^2 \leq 1\}.$$

Therefore, the complete locus \mathcal{S} is the union of these two components:

$$\mathcal{S} = \mathcal{R} \cup \mathcal{T}.$$

This locus \mathcal{S} is depicted in Figures 2b and 2d that visualize the changes in state vectors across the attention and MLP layers respectively.